SUPPLEMENTARY INFORMATION

Biodegradable calcium carbonate carriers for the topical delivery of clobetasol propionate

Mariia S. Saveleva[a], Roman A. Verkhovskii[a], Polina A. Demina[a], Yury I. Surkov[a,b], Roman A. Anisimov[a,b], Ekaterina S. Prikhozhdenko[a,b], Pavel S. Pidenko[c], Isabella A. Serebryakova[b], Sergey M. Zaytsev[b], Valery V. Tuchin[a,b], Yulia I. Svenskaya[a,*]

[a] Science Medical Center, Saratov State University, 410012 Saratov, Russia.
[b] Institute of Physics, Saratov State University, 410012 Saratov, Russia
[c] Institute of Chemistry, Saratov State University, 410012 Saratov, Russia
[*] Corresponding author: Yulia Svenskaya, e-mail: svenskaya@info.sgu.ru

Table SI 1. Loading capacity (LC) of various particulate formulations of clobetasol propionate

Drug formulation	DDS components	LC (%)	Reference
Sodium deoxycholate gel	- Sodium deoxycholate; - Mannitol;	0.05 (w/w)	1
Lecithin-chitosan nanoparticle suspension in chitosan gel	- Lecithin; - Chitosan;	0.005 (w/v)	
Lecithin/chitosan nanoparticles	- Lecithin; - Chitosan;	6.31 (w/w)	2
Lipid nanoparticles	- Lecithin; - Taurodeoxycholate; - Stearic acid; - Oleic acid;	2.34±0.1 (w/w)	3
Solid lipid nanoparticles	- Monostearin;	from 0.96 to 0.98 (w/w)	4
Solid lipid nanoparticles	- Monostearin;	2.63 ± 0.12	5
Nanostuctured lipid carriers	- Monostearin; - Caprylic/capric triglycerides;	3.48 ± 0.13	
Nanostuctured lipid carriers	- Compritol® ATO 888; - Oleic acid; - Poloxamer 188; - Sodium taurocholate;	from 12.38 ± 0.24 to 17.43 ± 0.17 (w/w)	6
Nanostructured lipid	- Stearic acid; - Oleic acid; - Lecithin;	1.26 ± 0.06 (w/w)	

carriers	- Sodium taurodeoxycholate;		[7]
	- Nanostructured lipid carriers coated with chitosan;	1.18 ± 0.03 (w/w)	
Nanostructured lipid carriers	- Lecithin; - Taurodeoxycholate; - Stearic acid; - Oleic acid;	0.99 ± 0.02 (w/w)	[8]
Nanostructured lipid carriers	- Stearic acid; - Oleic acid; - Lecithin; - Sodium taurodeoxycholate;	1.24±0.07 (w/w)	[9]
Nanoemulsion	- Eucalyptus oil; - Tween 20; - Ethanol;	0.05 (w/v)	[10]
Nanoemulsion gel	- Capmul MCM C8 EP; - Cremophor RH 40; - Labrafil 1944 CS;	0.05 (w/v)	[11]
Microemulsion	- Isopropyl myristate; - Cremophor EL; - Isopropyl alcohol;	0.5 (w/w)	[12]
Microemulsion based gel	- Microemulsion; - Carbopol 934P;	0.05 (w/w)	
Poly(-caprolactone) nanocapsules	- Poly(-caprolactone); - Polysorbate 80;	0.05 (w/v)	[13]
PLGA microspheres	- PLGA Mw 40,000; - PLGA Mw 75,000;	16.20±0.10 (w/w)	[14]
Hydrogel comprising cyclodextrin nanosponges	- β - cyclodextrin; - Diphenyl carbonate;	12.34±1.81 (w/w)	[15]
Gel incorporating drug-loaded squarticles	- PF68; -Squalene; - SPC; - Carbopol;	45.12 (w/v)	[16]

Method M1. Method for calculating the OCT signal attenuation coefficients

To assess the attenuation coefficient of the OCT signal in the follicle wall and follicle center, the attenuation coefficient of the probing irradiation was reconstructed using the method described in detail in Ref.[17] This method is based on the single scattering model and two assumptions: 1) almost all irradiation is attenuated within the depth range of the OCT scan; 2) backscattered light, which is recorded by the OCT system, is a fixed fraction of attenuated probing irradiation. These assumptions allow for estimation of attenuation coefficients for each pixel in the dataset without the necessity for a reference layer. Multiple scattered light was not taken into account. In accordance with this method, the attenuation coefficient - μ_{OCT} - was determined by the equation:

$$\mu_{OCT}(z) = \frac{I(z)}{\int_{z}^{D} I(u)du}, \quad (4)$$

where D is the range of the scanning depth of the OCT system, I(z) and I(u) are the intensity of the OCT signal at depths z and u, respectively.

Taking into account the discreteness of the OCT signal, equation (4) takes the form:

$$\mu_{OCT}(i) = \frac{1}{2\Delta} log\left(1 + \frac{I(i)}{\sum_{i+1}^{N} I(i)}\right), \quad (5)$$

where Δ is the pixel size, *I(i)* is the signal intensity of the i^{th} pixel, *N* is the number of pixels in the axial direction. The equation (5) was used to calculate the attenuation coefficient for each pixel in the depth profiles for each B-scan. To assess the attenuation coefficients of the OCT signal in the follicle wall and follicle center, the attenuation coefficients of the OCT signal were averaged in the selected ROI_1 and ROI_2.

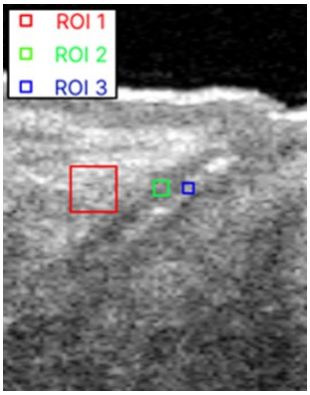

Figure M1. OCT image of the rat skin performed *in vivo* after the delivery of the CP-$CaCO_3$ carriers demonstrating the regions of interest: ROI_1 - dermis; ROI_2 - follicle wall; ROI_3 - follicle center

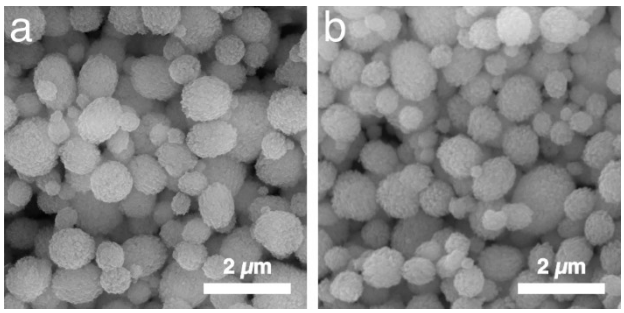

Figure SI 1. SEM images of the CP-$CaCO_3$ carriers demonstrating their stability upon storage in the dry state: the image obtained immediately after the carriers' preparation **(a)** and 13 months later **(b)**. The carriers were stored in a lidded tube in the fridge

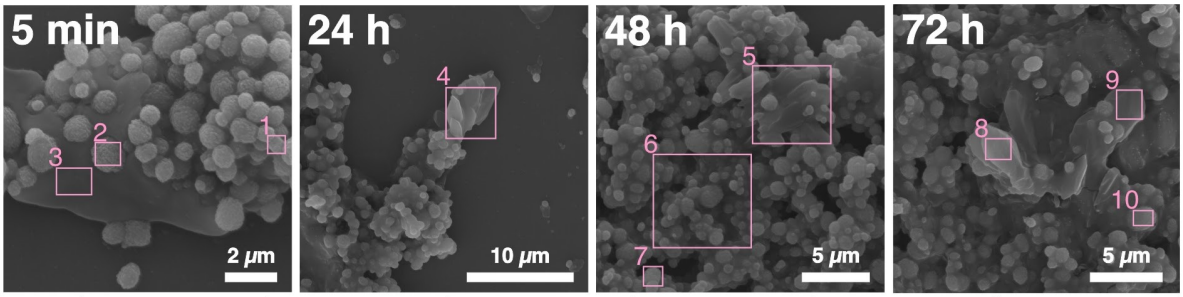

	C, W%	O, W%	F, W%	Ca, W%	Cl, W%	Na, W%
sp 1	35.0 ± 0.4	31.3 ± 0.3	0.0 ± 0.1	16.9 ± 0.1	9.8 ± 0.1	7.0 ± 0.1
sp 2	32.6 ± 0.4	30.8 ± 0.3	0.0 ± 0.1	13.1 ± 0.1	12.7 ± 0.1	10.8 ± 0.1
sp 3	30.5 ± 0.9	6.6 ± 0.2	0.0 ± 0.1	1.5 ± 0.1	40.3 ± 0.6	21.1 ± 0.3
sp 4	72.7 ± 0.5	16.3 ± 0.4	0.9 ± 0.2	3.0 ± 0.1	4.3 ± 0.1	2.8 ± 0.1
sp 5	58.7 ± 0.2	15.1 ± 0.2	0.7 ± 0.1	7.1 ± 0.1	11.1 ± 0.1	7.2 ± 0.1
sp 6	33.6 ± 0.3	30.6 ± 0.3	0.0 ± 0.1	20.8 ± 0.1	9.6 ± 0.1	5.5 ± 0.1
sp 7	26.0 ± 0.5	49.5 ± 0.5	0.0 ± 0.3	21.5 ± 0.3	0.8 ± 0.1	2.2 ± 0.1
sp 8	73.2 ± 0.2	16.6 ± 0.2	0.7 ± 0.1	5.1 ± 0.1	2.7 ± 0.0	1.8 ± 0.0
sp 9	65.6 ± 0.2	9.1 ± 0.2	0.7 ± 0.1	1.4 ± 0.0	13.2 ± 0.1	9.9 ± 0.1
sp 10	33.0 ± 0.3	40.3 ± 0.2	0.0 ± 0.1	16.6 ± 0.1	4.9 ± 0.1	5.2 ± 0.1

Figure SI 2. (**The upper panel**) - Characteristic SEM images of the CP-$CaCO_3$ carriers in the course of the incubation in DMEM at specific time points: 5 min, 24 h, 48 h and 72 h. The areas analyzed by EDX are pointed at SEM images. (**The bottom panel**) - The elemental composition of the sample in these areas, the data are presented in weight percent (w/w %).

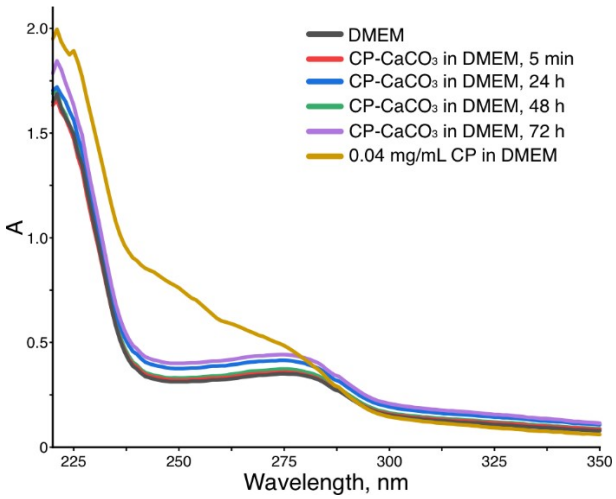

Figure SI 3. Absorption spectra of supernatants collected during the incubation of the CP-$CaCO_3$ carriers in DMEM at specific time points: 5 min, 24 h, 48 h and 72 h

a

Incubation time	Cumulative drug release
5 min	0 %
24 h	0 %
48 h	below threshold for quantification
72 h	6.8 ± 0.4 %

b

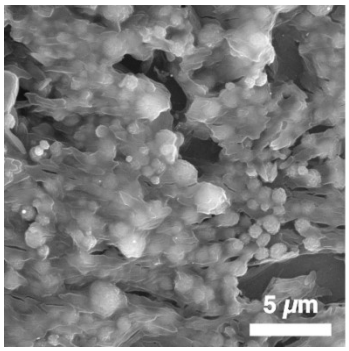

Figure SI 4. Cumulative release of CP from the CP-$CaCO_3$ carriers in DMEM containing the SDS (0.5 % w/v) during 72 h **(a)**. Characteristic SEM image of the CP-$CaCO_3$ carriers 72 h after their incubation in SDS-containing DMEM **(b)**

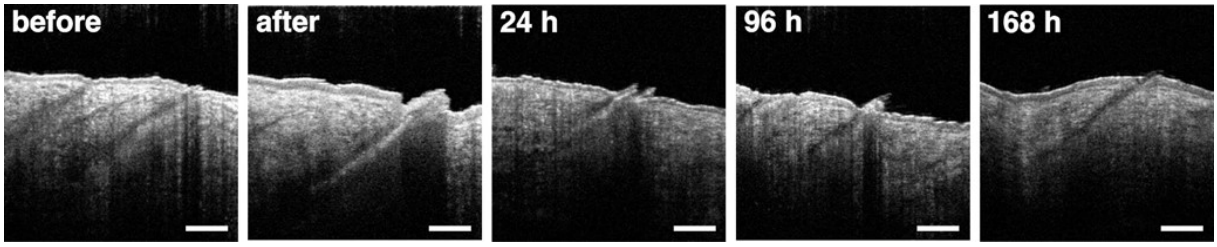

Figure SI 5. The unmarked version of Figure 6: characteristic OCT images of a rat skin with the well-defined hair follicles performed *in vivo* before and after the application of the CP-$CaCO_3$ carriers suspended in the mixture of PEG, oleic acid and propylene glycol (3.5:7.5:89 v/v, OCA 2) in the experimental site 2. The images obtained right after the carrier application and 24 h, 96 h and 168 h later illustrate gradual degradation of the CP-$CaCO_3$ carriers in hair follicles. The scale bars correspond to 250 µm

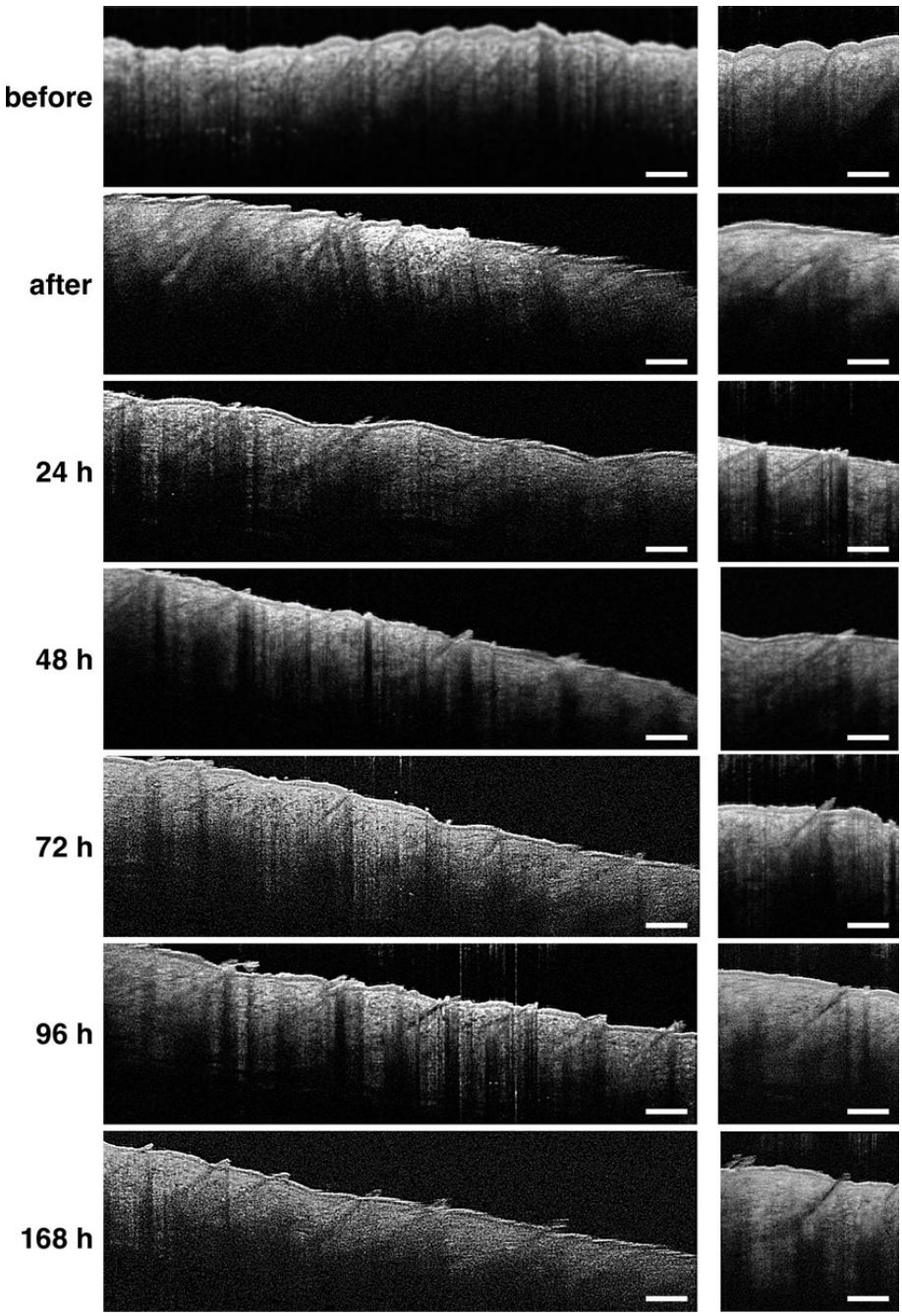

Figure SI 6. Characteristic OCT images of a rat skin with the well-defined hair follicles performed *in vivo* before and after the application of the CP-$CaCO_3$ carriers suspended in the mixture of PEG and oleic acid (80:20 v/v, OCA 1) in the experimental site 1. The images obtained right after the carrier application and at different time points further (24 h, 48 h, 72 h. 96 h and 168 h) illustrate gradual degradation of the CP-$CaCO_3$ carriers in hair follicles. The scale bars correspond to 250 μm

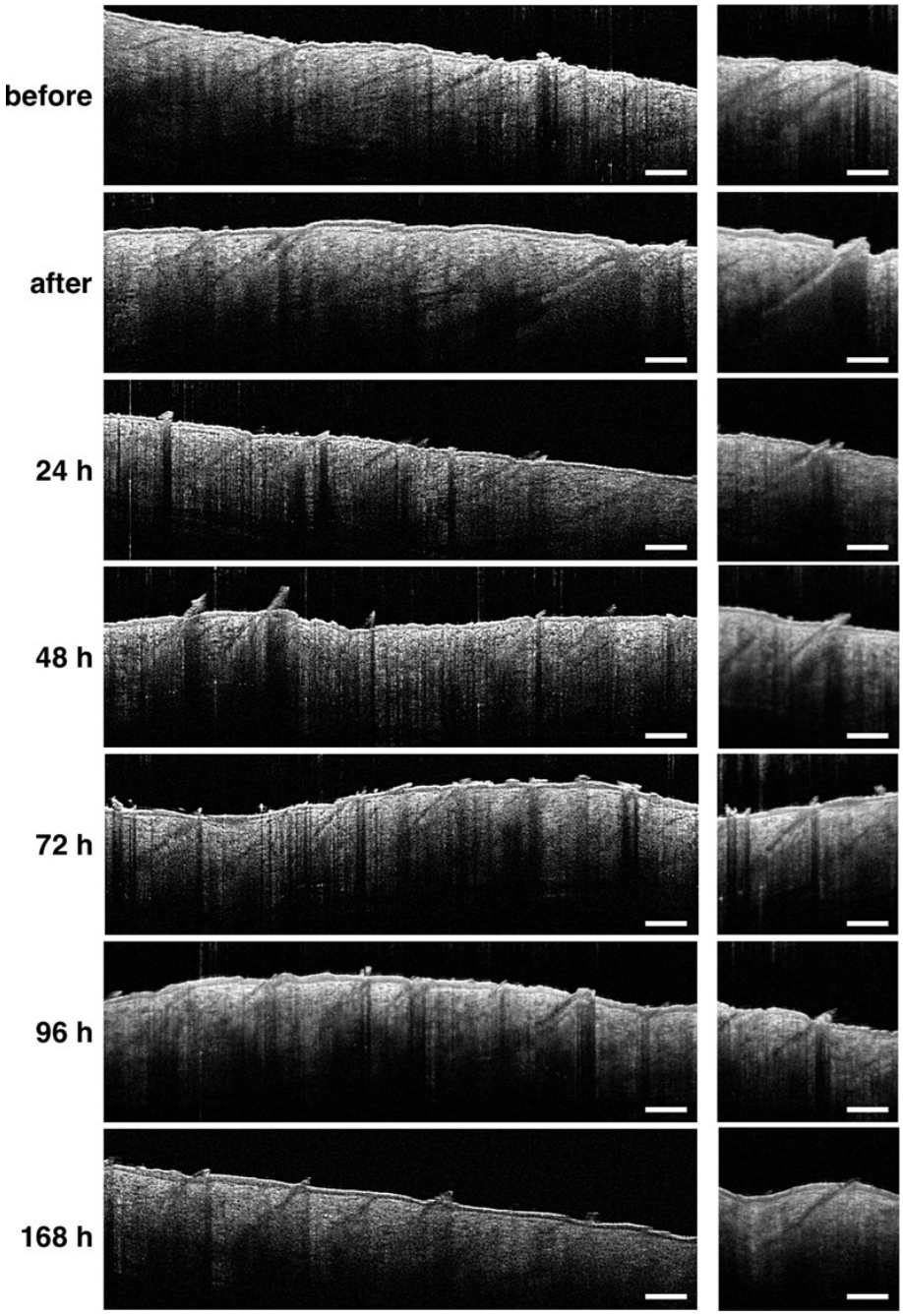

Figure SI 7. Characteristic OCT images of a rat skin with the well-defined hair follicles performed *in vivo* before and after the application of the CP-$CaCO_3$ carriers suspended in the mixture of PEG, oleic acid and propylene glycol (3.5:7.5:89 v/v, OCA 2) in the experimental site 2. The images obtained right after the carrier application and at different time points further (24 h, 48 h, 72 h. 96 h and 168 h) illustrate gradual degradation of the CP-$CaCO_3$ carriers in hair follicles. The scale bars correspond to 250 μm

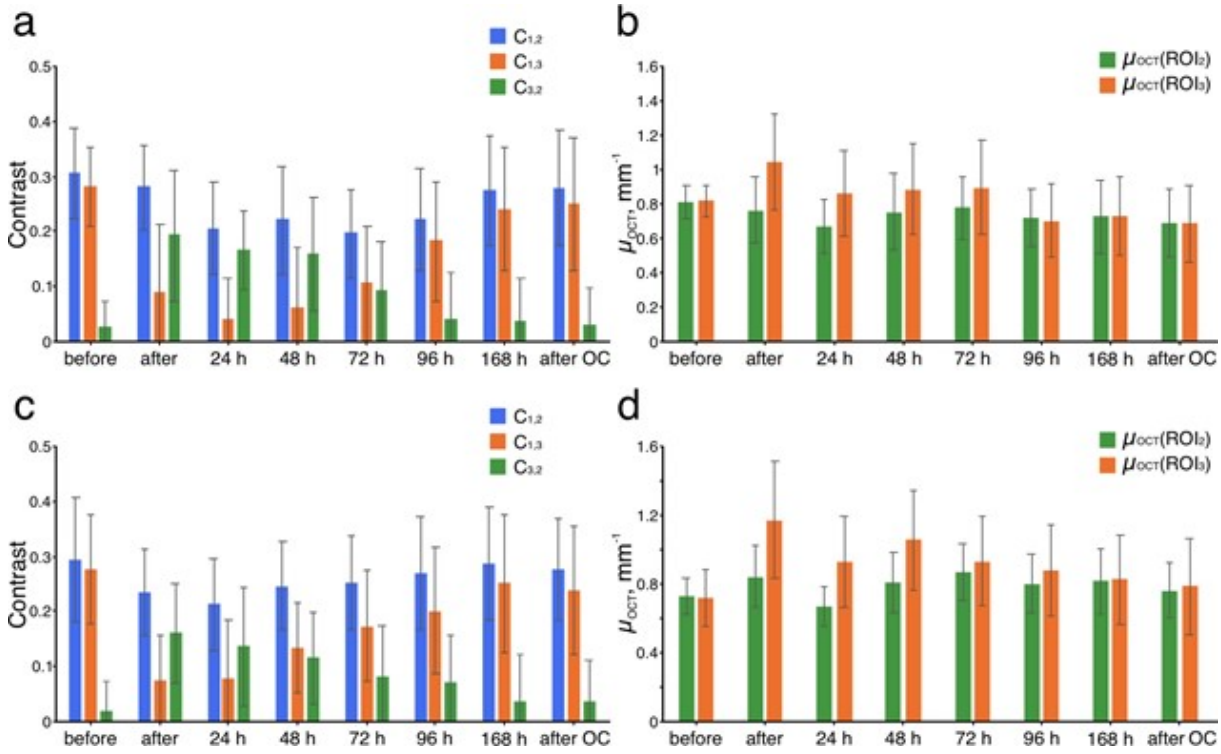

Figure SI 8. The change in OCT-image contrast values *C* (**a**) and attenuation coefficients of the OCT signal μ_{OCT} (**b**) at specific skin regions over time after the intrafollicular delivery of the CP-$CaCO_3$ carriers in the experimental site 1, where $C_{1,2}$ represents the image contrast between the adjacent dermis and the follicle wall, $C_{1,3}$ - between the dermis and the follicle center, $C_{3,2}$ - the follicle center and the follicle wall; $\mu_{OCT}(ROI_2)$ represents the OCT-signal attenuation coefficient in the area of follicle wall and $\mu_{OCT}(ROI_3)$ - in the follicle center. Analogical data is presented for experimental site 2 (**c** and **d**, respectively). The "after OC" time point corresponds to the OCA administration at the end of the observation (after 168 h)

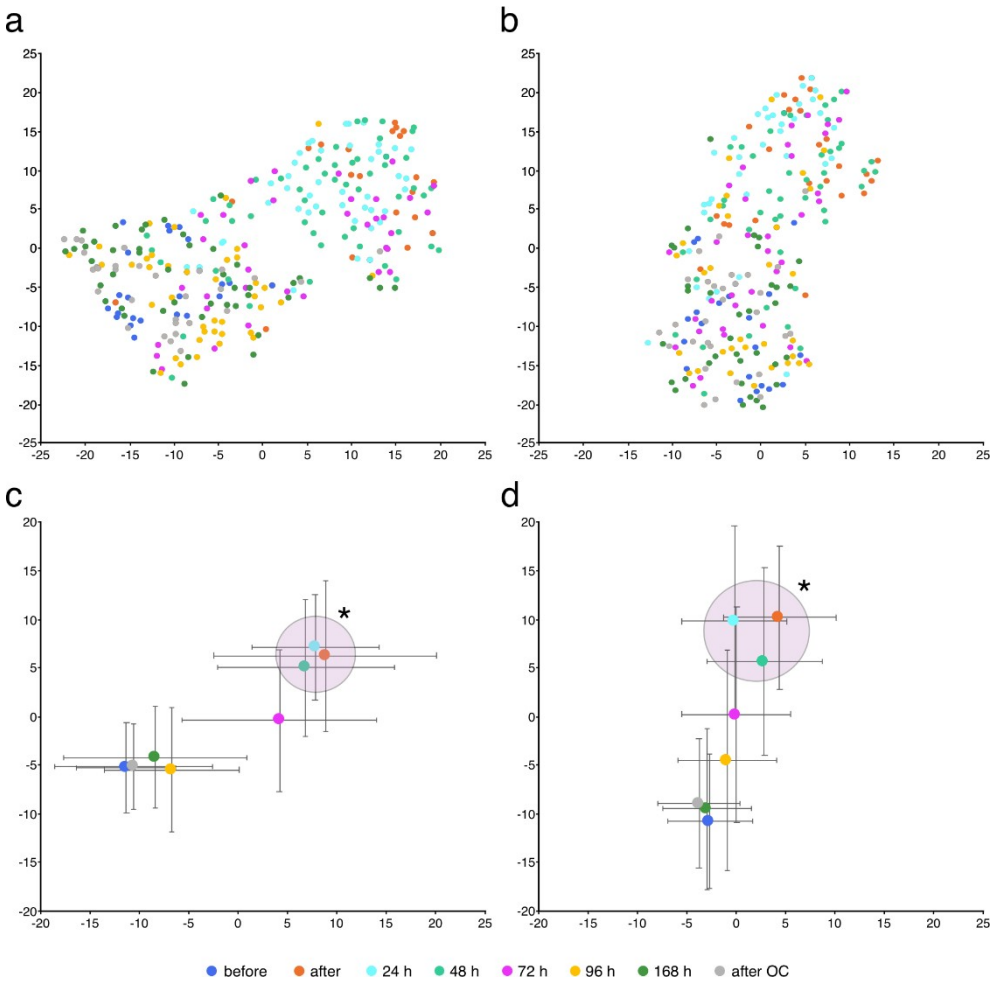

Figure SI 9. The two-dimensional t-SNE representation of the contrast and attenuation coefficients for the experimental sites 1 (**a**) and 2 **(b)**; and their average values represented as a "mean ± SD" for the experimental sites 1 (**c**) and 2 **(d)**. The data presented in graphs were calculated from the OCT images obtained before (before), right after the CP-$CaCO_3$ carriers' delivery (after) and at different time points further (24 h, 48 h, 72 h, 96 h, 168 h and after OC). The "after OC" time point corresponds to the OCA administration at the end of the observation (after 168 h). Pink circles marked with an asterisk (*) indicate the group of time points, where the differences in both t-SNE parameters in comparison with the control (obtained before the carriers' delivery) are significant ($P < 0.01$)

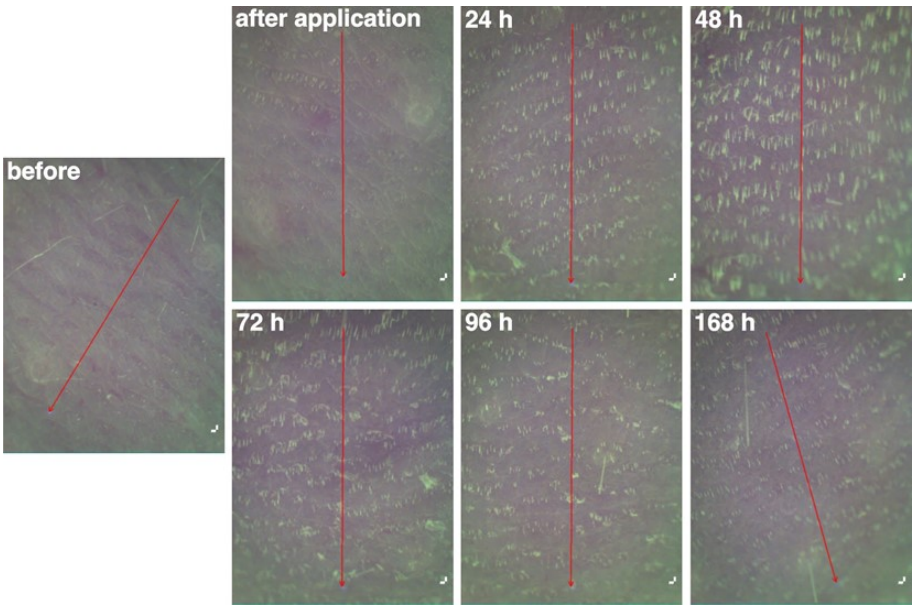

Figure SI 10. Photographs of a rat skin performed before and after the topical administration of the CP-$CaCO_3$ carriers (experimental site 1). The pixel size is 9 µm

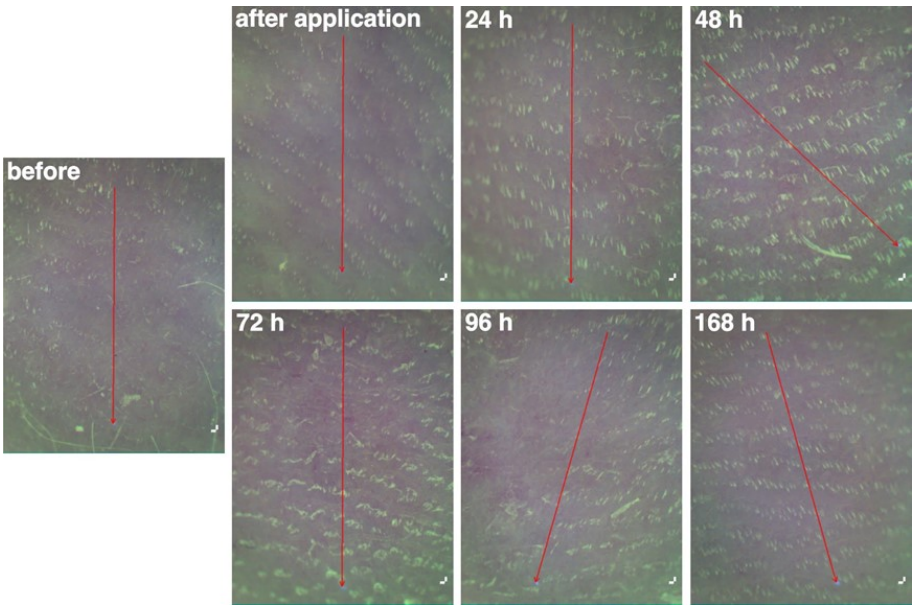

Figure SI 11. Photographs of rat skin performed before and after the topical administration of the CP-$CaCO_3$ carriers (experimental site 2). The pixel size is 9 µm

References

1 T. Şenyiğit, F. Sonvico, A. Rossi, I. Tekmen, P. Santi, P. Colombo, S. Nicoli and Ö. Özer, *Int J Mol Sci*, 2016, **18**, 32.

2 T. Şenyiğit, F. Sonvico, S. Barbieri, Ö. Özer, P. Santi and P. Colombo, *Journal of Controlled Release*, 2010, **142**, 368–373.

3 L. A. D. Silva, S. F. Taveira, E. M. Lima and R. N. Marreto, *Brazilian Journal of Pharmaceutical Sciences*, 2012, **48**, 811–817.

4 F. Q. Hu, H. Yuan, H. H. Zhang and M. Fang, *Int J Pharm*, 2002, **239**, 121–128.

5 F.-Q. Hu, S.-P. Jiang, Y.-Z. Du, H. Yuan, Y.-Q. Ye and S. Zeng, *Int J Pharm*, 2006, **314**, 83–89.

6 U. Nagaich and N. Gulati, *Drug Deliv Transl Res*, 2016, **6**, 289–298.

7 L. A. D. Silva, L. M. Andrade, F. A. P. de Sá, R. N. Marreto, E. M. Lima, T. Gratieri and S. F. Taveira, *Journal of Pharmacy and Pharmacology*, 2016, **68**, 742–750.

8 L. M. Andrade, L. A. D. Silva, A. P. Krawczyk-Santos, I. C. de S. M. Amorim, P. B. R. da Rocha, E. M. Lima, J. L. V. Anjos, A. Alonso, R. N. Marreto and S. F. Taveira, *European Journal of Pharmaceutics and Biopharmaceutics*, 2017, **119**, 142–149.

9 T. Angelo, N. El-Sayed, M. Jurisic, A. Koenneke, G. M. Gelfuso, M. Cunha-Filho, S. F. Taveira, R. Lemor, M. Schneider and T. Gratieri, *Sci Rep*, 2020, **10**, 176.

10 Md. S. Alam, Md. S. Ali, N. Alam, M. R. Siddiqui, Md. Shamim and M. M. Safhi, *Drug Invention Today*, 2013, **5**, 8–12.

11 A. Kaur, S. S. Katiyar, V. Kushwah and S. Jain, *Nanomedicine*, 2017, **13**, 1473–1482.

12 H. K. Patel, B. S. Barot, P. B. Parejiya, P. K. Shelat and A. Shukla, *Colloids Surf B Biointerfaces*, 2013, **102**, 86–94.

13 D. F. de Andrade, M. C. Fontana, A. R. Pohlmann, S. S. Guterres and R. C. R. Beck, *J Nanosci Nanotechnol*, 2015, **15**, 875–879.

14 U. Badıllı, T. Şen and N. Tarımcı, *AAPS PharmSciTech*, 2011, **12**, 949.

15 S. Kumar, M. Prasad and R. Rao, *Materials Science and Engineering: C*, 2021, **119**, 111605.

16 A. Dadwal, N. Mishra, R. K. Rawal and R. K. Narang, *J Microencapsul*, 2020, **37**, 341–354.

17 K. A. Vermeer, J. Mo, J. J. A. Weda, H. G. Lemij and J. F. de Boer, *Biomed Opt Express*, 2014, **5**, 322.